Research Paper

PAIN®

OPEN

Brainstem trigeminal fiber microstructural abnormalities are associated with treatment response across subtypes of trigeminal neuralgia

Sarasa Tohyama[a,b], Matthew R. Walker[a], Jia Y. Zhang[a], Joshua C. Cheng[c], Mojgan Hodaie[a,b,d,e,*]

Abstract

Neurosurgical treatments for trigeminal neuralgia (TN) can provide long-lasting pain relief; however, some patients fail to respond and undergo multiple, repeat procedures. Surgical outcomes can vary depending on the type of TN, but the reasons for this are not well understood. Neuroimaging studies of TN point to abnormalities in the brainstem trigeminal fibers; however, whether this is a common characteristic of treatment nonresponse across different subtypes of TN is unknown. Here, we used diffusion tensor imaging (DTI) to determine whether the brainstem trigeminal fiber microstructure is a common biomarker of surgical response in TN and whether the extent of these abnormalities is associated with the likelihood of response across subtypes of TN. We studied 98 patients with TN (61 classical TN, 26 TN secondary to multiple sclerosis, and 11 TN associated with a solitary pontine lesion) who underwent neurosurgical treatment and 50 healthy controls. We assessed treatment response using pain intensity measures and examined microstructural features by extracting pretreatment DTI metrics from the proximal pontine segment of the trigeminal nerves. We found that microstructural abnormalities in the affected pontine trigeminal fibers (notably, lower fractional anisotropy and higher radial diffusivity) highlight treatment nonresponders (n = 47) compared with responders (n = 51) and controls, and that the degree of abnormalities is associated with the likelihood of surgical response across subtypes of TN. These novel findings demonstrate the value of DTI as an objective, noninvasive tool for the prediction of treatment response and elucidate the features that distinguish treatment responders from nonresponders in the TN population.

Keywords: Trigeminal neuralgia, Facial pain, Lesion, Multiple sclerosis, Diffusion tensor imaging, Tractography, Treatment response

1. Introduction

Trigeminal neuralgia (TN) is a debilitating chronic facial pain disorder characterized by extremely intense, episodic, and electric shock–like attacks of unilateral pain.[12] To aid in diagnosis and treatment, TN is classified into different subtypes, including classical TN (CTN),[11,12] TN secondary to multiple sclerosis (MS-TN),[25] and more recently, TN associated with a solitary pontine lesion (SPL-TN).[37] The etiology and pathogenesis of these subtypes of TN range from peripheral to central theories. Classical TN often involves neurovascular compression of the trigeminal nerve at the root entry zone[23,27]; MS-TN is commonly associated with multiple, diffuse, demyelinating pontine plaques[4]; and SPL-TN is defined by a single, distinct pontine lesion along the trigeminal nerve pathway and no other supratentorial or infratentorial lesions.[37] Importantly, the treatment outcomes across these subtypes of TN differ considerably. Classical TN patients experience the highest response rates to surgical treatment, with approximately 70% to 80% of patients achieving long-term pain relief (ie, > 1 year).[7,14,19,26,28,32] MS-TN patients are less amenable to surgical treatment, with approximately 50% to 80% of patients experiencing long-term pain relief.[8,40,42] Finally, SPL-TN patients are believed to respond the least (~5% responders) and are collectively considered nonresponders to surgical treatment.[37]

Although there is a clear gradient of treatment response across the subtypes of TN, the reason why one group responds better than another is unknown. A promising approach to investigate this gap in knowledge is diffusion tensor imaging (DTI), which offers a noninvasive, in vivo means to probe brain white matter microstructure.[1] The most widely used DTI metric for quantitative microstructural assessment is fractional anisotropy (FA), which is believed to reflect overall white matter microstructure or "integrity."[29] Other metrics that complement FA include radial diffusivity (RD), axial diffusivity (AD), and mean diffusivity (MD), which have been shown to specifically reflect myelination,[33,35] axonal integrity,[34] and neuroinflammation,[1] respectively. There is growing interest and success in using DTI to study TN, including examination of the underlying pathophysiological mechanisms,[3,5,6,13,20,22,39,41] and its clinical application in neurosurgical platforms.[16,17,21,36] Notably, multitensor

Sponsorships or competing interests that may be relevant to content are disclosed at the end of this article.

[a] Division of Brain, Imaging, and Behaviour—Systems Neuroscience, Krembil Research Institute, Toronto Western Hospital, University Health Network, Toronto, ON, Canada, [b] Institute of Medical Science, Faculty of Medicine, University of Toronto, Toronto, ON, Canada, [c] Stony Brook University School of Medicine, Stony Brook, NY, United States, [d] Department of Surgery, Faculty of Medicine, University of Toronto, Toronto, ON, Canada, [e] Division of Neurosurgery, Krembil Neuroscience Centre, Toronto Western Hospital, University Health Network, Toronto, ON, Canada

**Corresponding author. Address: Division of Neurosurgery, Toronto Western Hospital, 399 Bathurst St, 4W W-443, Toronto, ON, Canada M5T 2S8. Tel.: (416) 603-6441; fax: (416) 603-5298. E-mail address: mojgan.hodaie@uhn.ca (M. Hodaie).*

PAIN 162 (2021) 1790–1799

http://dx.doi.org/10.1097/j.pain.0000000000002164

diffusion tractography has enabled detailed visualization of the brainstem trigeminal fibers, allowing assessment of both the peripheral and central (brainstem) components of the trigeminal nerve pathway.[2,3] Using these techniques in the context of treatment response, isolated studies on CTN, MS-TN, and SPL-TN have all pointed toward centrally disrupted brainstem trigeminal fibers as a key characteristic of treatment nonresponders.[16,21,37] Thus, it is plausible that the clinical response spectrum across these subtypes of TN may be associated with the extent of microstructural alterations of the brainstem trigeminal fibers.

The aim of the current study was to investigate whether there is a common DTI-based biomarker of surgical response across subtypes of TN. We hypothesized that DTI metrics of the affected brainstem trigeminal fibers will distinguish treatment responders from nonresponders in a large cohort of TN patients. Specifically, nonresponders will demonstrate microstructural abnormalities, characterized by lower FA and higher RD, AD, and MD compared with responders and healthy controls. We also hypothesized that the degree of microstructural abnormalities will be associated with the likelihood of surgical response across subtypes of TN.

2. Materials and methods

2.1. Participants

This study included 98 patients with TN (39 men and 59 women, mean age ± SD: 58.3 ± 13.8 years) and 50 healthy controls (24 men and 26 women, mean age ± SD: 53.1 ± 13.1 years). Patients were identified through retrospective record reviews and consisted of the following subtypes of TN: 61 CTN, 26 MS-TN, and 11 SPL-TN. Healthy controls were recruited from the public through advertisements and were age-/sex-matched to each patient group. The inclusion criteria for patients were the following: (1) diagnosis of CTN or MS-TN according to the International Classification of Headache Disorders-3[11] or diagnosis of SPL-TN according to our recent study defining this new syndrome[37] (all SPL-TN patients included in the current study were used in this prior study), (2) between the ages of 18 and 80 years, (3) underwent neurosurgical treatment for TN at the Toronto Western Hospital, University Health Network (Toronto, Ontario, Canada), (4) a minimum clinical follow-up of 6 months, and (5) a magnetic resonance imaging (MRI) session consisting of a high-resolution anatomical and diffusion weighted imaging (DWI) scan. A range of neurosurgical treatments were performed, including microvascular decompression (MVD) surgery, Gamma Knife radiosurgery (GKRS), and percutaneous trigeminal rhizotomy (PTR). The specifics of these procedures are provided in our previous works.[14,36] The inclusion criteria for healthy controls were the following: (1) no prior record of neurological, psychiatric, or pain disorders, (2) no prior major operation of the central nervous system, and (3) no contraindications for an MRI scan. All study procedures were approved by the University Health Network Research Ethics Board, and healthy control participants provided written informed consent.

2.2. Classification of treatment response

Clinical follow-up data were retrospectively reviewed to classify each patient as a responder or nonresponder to neurosurgical treatment. The primary outcome measure of pain intensity was assessed using 2 scales: (1) the Numerical Rating Scale (0: no pain; 10: worst possible pain) and (2) the Barrow Neurological Institute (BNI) scale (I: no trigeminal pain, no medication; II: occasional pain, no medication; III: some pain, adequately controlled with medication; IV: some pain, not adequately controlled with medication; and V: severe pain, no pain relief). Patients were classified as responders if they reported ≥75% reduction in pain intensity and a BNI score of I to III for ≥12 months after treatment. Patients were classified as nonresponders if they did not meet the above criteria (ie, <75% reduction in pain intensity within 12 months and a BNI score of IV or V) or had undergone multiple, repeat treatments (ie, ≥3 surgeries) because of inadequate pain relief. These benchmarks of successful neurosurgical response have been repeatedly used in TN research.[6,17,19,21,36,37] Other clinical characteristics, including age of onset of TN, pain duration, pain laterality (right-sided or left-sided pain), and pain distribution (V1–3) were also collected for each patient at the pretreatment time point.

2.3. Magnetic resonance imaging acquisition

Both patients and healthy controls underwent an MRI session using the same 3T GE MR scanner, equipped with an 8-channel phased-array head coil. High-resolution T1-weighted FSPGR anatomical images (voxel size = $0.94 \times 0.94 \times 1$ mm^3, matrix = 256×256, repetition time = 12 ms, echo time = 5.1 ms, inversion time = 300 ms, flip angle = 20°, and field of view = 24 cm) and diffusion-weighted images (60 directions, spin echo EPI sequence, 1 B_0, b = 1000 s/mm^2, 1 excitation, ASSET, voxel size = $0.94 \times 0.94 \times 3$ mm^3, matrix = 256×256, repetition time = 12,000 ms, echo time = 86.4 ms, flip angle = 90°, and field of view = 24 cm) were collected. For the patients, T1-weighted FLAIR images (voxel size = $0.43 \times 0.43 \times 3$ mm^3, matrix = 512×512, repetition time = 2367 ms, echo time = 13 ms, inversion time = 860 ms, echo train length = 6, and flip angle = 90°) and T2-weighted FIESTA images (voxel size = $0.39 \times 0.39 \times 0.80$ mm^3, matrix = 512×512, repetition time = 4.5 ms, echo time = 2.2 ms, and flip angle = 37°) were also collected. For the CTN and MS-TN group, the pretreatment (surgically naïve) imaging time point was used. For the SPL-TN group, the earliest available imaging time point was used, given their extremely refractory nature and history of having undergone multiple surgical procedures. Of the 11 SPL-TN patients, 2 had surgically naïve DWI scans. This limitation has been previously addressed in our study through additional data analysis and discussion.[37]

2.4. Assessment of neurovascular contact

The presence of neurovascular contact was evaluated for each patient using T2-weighted FIESTA images. Both the affected and unaffected sides of the trigeminal nerves were examined. Two SPL-TN patients with a history of MVD were excluded from this assessment.

2.5. Diffusion-weighted imaging processing

For the diffusion-weighted images, distortions because of eddy currents and subject motion were corrected in FSL v5.0.[18] Then, diffusion tensor estimation and scalar map calculation were performed in 3D Slicer v4.3.1.[9] This process generated a diffusion tensor image and corresponding scalar maps (ie, maps of FA, RD, AD, and MD) for each participant. Next, linear registration was performed to transform each participant's T1-weighted anatomical image to DWI space. This was performed manually in 3D Slicer, to emphasize alignment of both the trigeminal nerves and midpontine region of the brainstem.

2.6. Multitensor diffusion tractography

The trigeminal nerve fibers, including the brainstem trigeminal fibers, were reconstructed using eXtended Streamline Tractography (XST)[31] (**Fig. 1**). This deterministic tractography algorithm is based on

a constrained 2-tensor model, which aims to resolve crossing fibers within clinically practical scan times.[30] The advancement of XST has facilitated reconstruction of white matter tracts previously indiscernible using the traditional single-tensor model because of fiber crossings, such as the brainstem trigeminal fibers.[3] For each participant, fiber tracts were generated from seeds placed manually on both sides of the trigeminal root entry zone in axial view in 3D Slicer. Tracking parameters were the following: Westin planar threshold = 0.2, tensor fraction = 0.2, radius of curvature = 0.8 mm, minimum length = 10 mm, and step size = 1 mm. Of 150 eligible participants, 2 patients were excluded for failure to reconstruct the brainstem trigeminal fibers on both sides.

2.7. Region of interest definition and microstructural analysis

Diffusion tensor metrics of FA, RD, AD, and MD were extracted from the proximal pontine segment of the trigeminal nerves in 3D Slicer by one of the authors (S.T.), who was blinded to treatment response group allocation (**Fig. 1**). Region of interest (ROI) placement was accomplished manually for each participant using a tractography-guided approach. After reconstruction of the trigeminal nerve fibers using XST (as described above), the proximal portion of the brainstem trigeminal fibers was visualized in the axial plane. In 90.2% of cases (267/296 tracts), this corresponded to one slice below (in the z-direction) the slice where the trigeminal nerves were visualized entering the pons. In the same axial view, a ROI covering 4 voxels was placed at the most proximal portion of the brainstem trigeminal fibers, in close proximity to the trigeminal brainstem sensory nuclear complex (VBSNC). This typically coincided with where the tracts truncated or curved centrifugally towards a ~90° angle. The ROI size of 4 voxels has been previously used to capture diffusivity changes in the pontine segment of the trigeminal nerve.[16,21] To further account for the stability of the ROI location and partial volume effects, all ROIs were placed in the green zone of the diffusion tensor image (ie, the voxels where the major eigenvector is in the anterior–posterior orientation), consistent with the anatomy of the trigeminal afferent fibers moving in the anterior to posterior direction before descending down along the spinal trigeminal tract (in the superior to inferior direction) and terminating onto the VBSNC. In the patient group, ROIs were defined based on pain laterality, such that the affected ROI corresponded to the painful side and the unaffected ROI corresponded to the nonpainful side. In the healthy control group, the left and right ROIs were averaged across each individual.

To determine whether DTI as a modality can distinguish treatment responders from nonresponders in TN in general, DTI metrics were compared between all treatment responders and nonresponders (regardless of the subtype of TN), as well as healthy controls. Then, to determine whether the degree of brainstem trigeminal fiber microstructural abnormalities is associated with the likelihood of surgical response across subtypes of TN, DTI metrics were compared between each subgroup (CTN, MS-TN, and SPL-TN) of responders and nonresponders. Furthermore, these metrics were compared against the contralateral, unaffected side and healthy controls.

2.8. Statistical analysis

Differences between groups were assessed using independent samples t-tests or 1-way analysis of variance (ANOVA), whereas differences within groups were assessed using paired-samples *t*-tests. Relationships between continuous variables were assessed using Pearson's correlations, whereas categorical variables were assessed using the χ^2 test. Normality of the data was assessed using the Shapiro–Wilk test. For nonnormally distributed variables, a nonparametric equivalent test was performed. If the data had unequal variances (determined by Levene's test for homogeneity of variances) and/or unequal sample sizes, Welch's *t* test or Welch's ANOVA followed by Games–Howell post-hoc tests was performed. For multiple testing correction, false discovery rate correction using the Benjamini–Hochberg method was applied for the 4 DTI metrics for each separate analysis. Statistical analyses were performed in SPSS v22.0 (IBM, Armonk, NY), with a statistical significance criterion of $P < 0.05$ or $q < 0.05$ (ie, false discovery rate adjusted *P*-value).

3. Results

Overall, the study comprised 51 responders (19 men and 32 women, mean age ± SD: 58.7 ± 14.0 years), 47 nonresponders (20 men and 27 women, mean age ± SD: 57.8 ± 13.7 years), and 50 age-/sex-matched healthy controls (24 men and 26 women, mean age ± SD: 53.1 ± 13.1 years). There were no statistically significant differences in age ($\chi^2(2) = 4.56$, $P = 0.10$) or sex ($\chi^2(2) = 1.19$, $P = 0.55$) between the 3 groups. There were also no significant differences in age of onset of TN (mean age of TN onset ± $SD_{responders}$ = 51.8 ± 11.8 years, mean age of TN onset ±

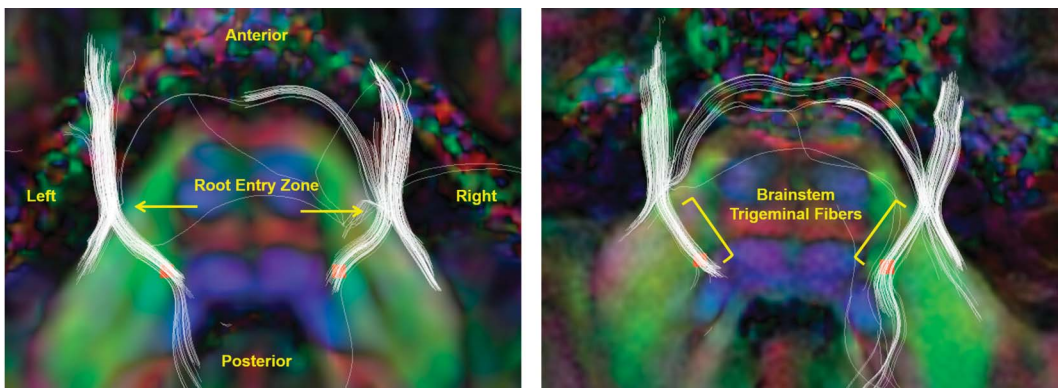

Figure 1. Multitensor diffusion tractography of the trigeminal nerves and ROI placement. Panels represent tractography of the trigeminal nerves (in white) and ROI placement at the proximal pontine segment (in red) in axial view for 2 example participants. The fiber tracts are superimposed on coregistered semitransparent T1-weighted anatomical and underlying diffusion tensor images. The diffusion tensor images are colored by orientation (red, left–right; green, anterior–posterior; and blue, superior–inferior). (Left panel) Arrows indicate the root entry zone of the trigeminal nerve, where tractography is generated from. (Right panel) Brackets indicate the brainstem trigeminal fibers, which are used to guide ROI placement at the proximal pontine segment for DTI metric extraction. DTI, diffusion tensor imaging; ROI, region of interest.

$SD_{nonresponders}$ = 49.7 ± 11.5 years; U = 951.5, P = 0.52) and pain duration (mean number of years ± $SD_{responders}$ = 7.5 ± 7.9 years, mean number of years ± $SD_{nonresponders}$ = 7.5 ± 7.4 years; U = 1014, P = 0.89) between responders and nonresponders.

3.1. Microstructural diffusion tensor metrics distinguish treatment responders from nonresponders in trigeminal neuralgia

There was a statistically significant difference between responder, nonresponder, and healthy control groups as determined by Welch's ANOVA in FA ($F(2, 93.90) = 14.26$, $P = 4.0 \times 10^{-6}$), RD ($F(2, 90.86) = 7.22$, $P = 0.0012$), and AD ($F(2, 95.89) = 9.25$, $P = 2.1 \times 10^{-4}$). There was no significant difference in MD between groups ($F(2, 89.50) = 1.40$, $P = 0.25$). A Games–Howell post-hoc test revealed significantly higher FA in responders ($P = 3.6 \times 10^{-5}$) and healthy controls ($P = 7.0 \times 10^{-6}$) compared with nonresponders. Radial diffusivity was significantly lower in responders ($P = 0.0021$) and healthy controls ($P = 0.0014$) compared with nonresponders. Axial diffusivity was significantly higher in responders ($P = 0.043$) and healthy controls ($P = 1.7 \times 10^{-4}$) compared with nonresponders. There was no significant difference between responders and healthy controls in FA, RD, and AD ($P > 0.05$) (**Fig. 2**). In healthy controls, there were no significant differences between the left and right nerves in FA, RD, AD, and MD ($q > 0.05$).

3.2. Spectrum of clinical response across subtypes of trigeminal neuralgia

Of the 3 subtypes of TN examined, CTN patients had the highest response rate to surgical treatment, followed by MS-TN patients, and, finally, SPL-TN patients (**Fig. 3**). In the CTN group, 39 of 61 patients (63.9%) were identified as responders to surgical treatment. In the MS-TN group, 11 of 26 patients (42.3%) were identified as responders, whereas only 1 patient of the 11 patients with SPL-TN (9.1%) was deemed a responder. The demographic and clinical characteristics of each of the subtype/response groups are presented in **Table 1**.

3.3. Brainstem trigeminal fiber microstructural abnormalities are associated with the likelihood of surgical response across subtypes of trigeminal neuralgia

In responders, there were no statistically significant differences between the 2 subtypes of TN (CTN and MS-TN) in FA ($t_{(15.58)} = 1.33$, $q = 0.39$), RD ($t_{(15.56)} = -0.27$, $q = 0.80$), MD ($t_{(12.78)} = 1.10$, $q = 0.39$), and AD ($t_{(13.98)} = 1.86$, $q = 0.34$) (**Figs. 4A–D**). The SPL-TN group was not included in this analysis because there was only 1 responder. There were no significant differences in age ($t_{(20.03)} = 1.86$, $P = 0.077$), sex ($\chi^2(1) = 0.33$, $P = 0.56$), age of onset of TN ($t_{(13.68)} = 1.07$, $P = 0.30$), or pain duration ($t_{(25.18)} = 1.44$, $P = 0.16$) between CTN and MS-TN responders (corresponding descriptive statistics are presented in **Table 1**).

In nonresponders, there was a statistically significant difference between CTN, MS-TN, and SPL-TN groups as determined by Welch's ANOVA in FA ($F(2, 20.96) = 27.51$, $P = 1.0 \times 10^{-6}$), RD ($F(2, 17.46) = 19.57$, $P = 3.5 \times 10^{-5}$), and MD ($F(2, 17.61) = 12.00$, $P = 5.2 \times 10^{-4}$). There was no significant difference in AD between groups ($F(2, 20.98) = 0.57$, $P = 0.57$). A Games–Howell post-hoc test revealed significantly higher FA in CTN patients ($P = 5.0 \times 10^{-6}$) and MS-TN patients ($P = 0.011$) compared with SPL-TN patients. Classical TN patients also had significantly higher FA ($P = 0.042$) compared with MS-TN patients. Radial diffusivity was significantly lower in CTN patients ($P = 1.9 \times 10^{-4}$) and MS-TN patients ($P = 0.0075$) compared with SPL-TN patients, but no significant differences were found between CTN and MS-TN patients ($P = 0.13$). Mean diffusivity was also significantly lower in CTN patients ($P = 0.0013$) and MS-TN patients ($P = 0.018$) compared

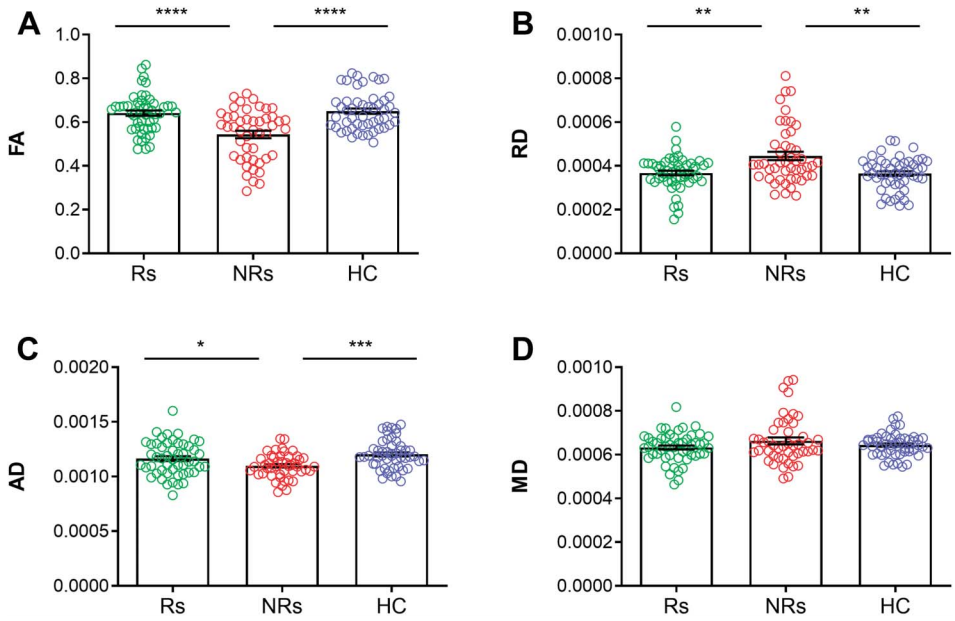

Figure 2. Diffusion tensor imaging–based biomarker of surgical response in trigeminal neuralgia. Mean DTI metrics (±SEM) of responders (green), nonresponders (red), and healthy controls (blue). The brainstem trigeminal fiber microstructure is significantly altered in nonresponders compared with responders and healthy controls as shown by changes in FA (A), RD (B), and AD (C). No differences were found in MD (D). The microstructural characteristics of responders are comparable with that of healthy controls, with no significant differences between the 2 groups for all 4 DTI metrics (A–D). *$P < 0.05$, **$P < 0.01$, ***$P < 0.001$, ****$P < 0.0001$ (multiple comparison corrected). AD, axial diffusivity; DTI, diffusion tensor imaging; FA, fractional anisotropy; HC, healthy controls; MD, mean diffusivity; NRs, nonresponders; RD, radial diffusivity; Rs, responders.

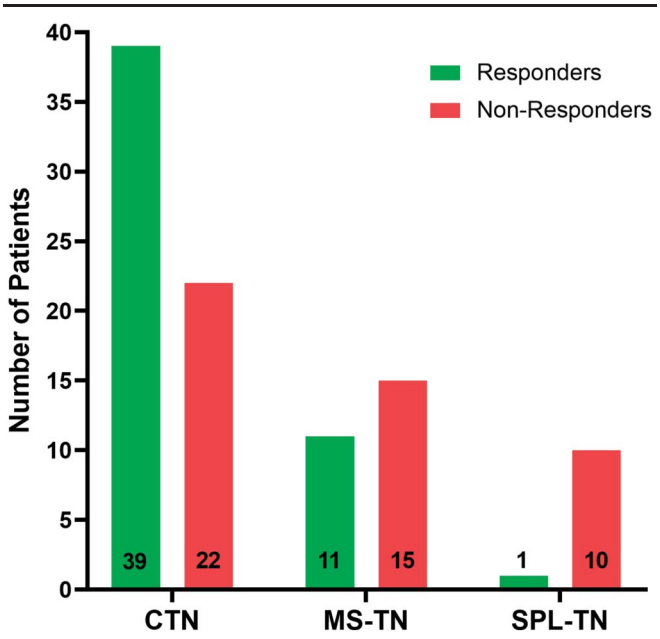

Figure 3. Spectrum of clinical response. Bar graphs showing the number of responders (green) and nonresponders (red) in each subgroup of TN. CTN, classical TN; MS-TN, TN secondary to multiple sclerosis; SPL-TN, TN associated with solitary pontine lesion; TN, trigeminal neuralgia.

with SPL-TN patients, and no significant differences were found between CTN and MS-TN patients ($P = 0.36$) (**Figs. 4E–H**). There was a significant difference between groups as determined by Welch's ANOVA in age ($F(2, 28.39) = 12.68$, $P = 1.2 \times 10^{-4}$) and pain duration ($F(2, 18.76) = 4.29$, $P = 0.029$). However, appropriate Pearson's or Spearman's correlations determined that there were no significant correlations between each DTI metric (FA, RD, MD, and AD) and age as well as pain duration within the 3 nonresponder subgroups, respectively ($q > 0.05$). A 1-way ANCOVA could not be performed to statistically control for age and pain duration because of unequal variances and sample sizes. There were no significant differences in sex ($\chi^2(2) = 4.66$, $P = 0.098$) and age of onset of TN ($F(2, 22.75) = 1.31$, $P = 0.29$) between groups (corresponding descriptive statistics are presented in **Table 1**).

Both CTN and MS-TN responders had no statistically significant differences between the affected vs unaffected side, affected side vs healthy controls, and unaffected side vs healthy controls for all 4 DTI metrics ($q > 0.05$ for all comparisons) (**Figs. 5A–D**). Classical TN nonresponders also had no statistically significant differences between the affected vs unaffected side, affected side vs healthy controls, and unaffected side vs healthy controls for all 4 DTI metrics ($q > 0.05$ for all comparisons). In MS-TN nonresponders, the affected and unaffected side did not significantly differ in FA, RD, MD, and AD ($q > 0.05$). Compared with healthy controls, the affected side had significantly lower FA ($t_{(28)} = -3.04$, $q = 0.020$), but no changes were found in RD ($t_{(28)} = 1.92$, $q = 0.087$), MD ($t_{(19.37)} = 0.55$, $q = 0.59$), and AD ($t_{(28)} = -2.16$, $q = 0.079$). There were no significant differences between the unaffected side and healthy controls in FA, RD, MD, and AD ($q > 0.05$). In SPL-TN nonresponders, the affected side had significantly lower FA ($t_{(9)} = -7.99$, $q = 8.8 \times 10^{-5}$) and higher RD ($t_{(9)} = 6.07$, $q = 3.7 \times 10^{-4}$) and MD ($t_{(9)} = 3.26$, $q = 0.013$) compared with the unaffected side. No differences were found in AD ($t_{(9)} = -0.49$, $q = 0.64$). Compared with healthy controls, the affected side demonstrated the same pattern of significantly lower FA ($t_{(18)} = -7.06$, $q = 4.0 \times 10^{-6}$), and higher RD ($t_{(13.13)} = 5.26$, $q = 3.0 \times 10^{-4}$) and MD ($t_{(12.88)} = 3.73$, $q = 0.0034$), with no changes in AD ($U = 47$, $q = 0.82$). There were no significant differences between the unaffected side and healthy controls in FA, RD, MD, and AD ($q > 0.05$) (**Figs. 5E–H**). There were no significant differences in age or sex between patients and controls for all 5 subgroups ($P > 0.05$).

4. Discussion

This study reveals, for the first time, a common DTI-based biomarker of surgical response across different subtypes of TN. Our key findings were that (1) DTI metrics of the affected brainstem trigeminal fibers can distinguish treatment responders from nonresponders in a large, mixed cohort of TN patients, (2) there is

Table 1

Demographic and clinical characteristics of trigeminal neuralgia subtypes.

Treatment response	CTN		MS-TN		SPL-TN	
	39 Rs	22 NRs	11 Rs	15 NRs	1 R	10 NRs
Age	60.0 ± 14.2	55.1 ± 15.1	52.5 ± 11.2	54.2 ± 12.0	78	69.0 ± 5.5
Sex	14 M, 25 F	9 M, 13 F	5 M, 6 F	4 M, 11 F	1 F	7 M, 3 F
TN onset age	52.4 ± 12.2	48.1 ± 12.9	48.1 ± 10.4	48.7 ± 10.2	61	54.6 ± 9.5
Pain duration	7.8 ± 8.5	6.1 ± 6.2	5.0 ± 4.3	4.9 ± 4.7	17	14.8 ± 9.2
Pain laterality	27 R, 12 L	10 R, 12 L	7 R, 4 L	5 R, 10 L	1 L	4 R, 6 L
Pain distribution	3 V1, 4 V2, 4 V3, 4 V1/2, 17 V2/3, 0 V1/3, 7 V1/2/3	0 V1, 1 V2, 3 V3, 5 V1/2, 7 V2/3, 1 V1/3, 5 V1/2/3	0 V1, 2 V2, 2 V3, 1 V1/2, 3 V2/3, 0 V1/3, 3 V1/2/3	0 V1, 0 V2, 8 V3, 1 V1/2, 5 V2/3, 0 V1/3, 1 V1/2/3	1 V2/3	0 V1, 0 V2, 3 V3, 1 V1/2, 5 V2/3, 0 V1/3, 1 V1/2/3
First-line surgical treatment	27 GKRS, 11 MVD, 1 PTR	17 GKRS, 5 MVD	11 GKRS	14 GKRS, 1 PTR	1 GKRS	3 GKRS, 1 MVD, 6 PTR*
Neurovascular contact	37 Aff, 18 Unaff	15 Aff, 4 Unaff	8 Aff, 6 Unaff	5 Aff, 5 Unaff	0 Aff, 0 Unaff	4 Aff, 5 Unaff†

All values given in numbers or mean years (±SD).

* SPL-TN patients are refractory to surgical management and have undergone multiple procedures without clinical benefit.[37]

† Two SPL-TN patients were excluded from assessment of neurovascular contact because of a history of MVD.

Aff, affected side; CTN, classical trigeminal neuralgia; F, female; GKRS, Gamma Knife radiosurgery; L, left; M, male; MVD, microvascular decompression; MS-TN, TN secondary to multiple sclerosis; NRs, nonresponders; PTR, percutaneous trigeminal rhizotomy; R, right; Rs, responders; SPL-TN, TN associated with solitary pontine lesion; TN, trigeminal neuralgia; Unaff, unaffected side; V1, ophthalmic branch; V2, maxillary branch; V3, mandibular branch.

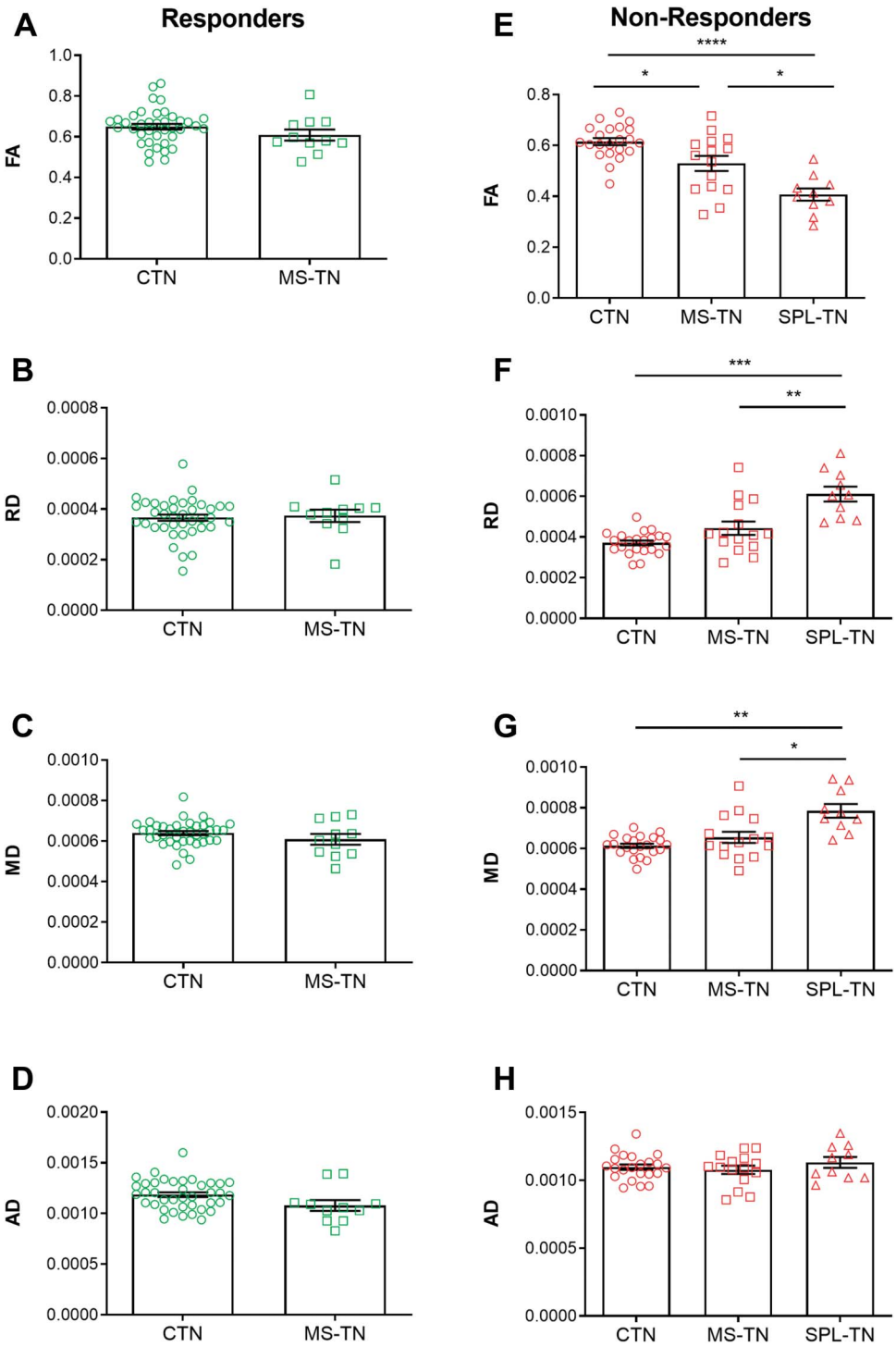

Figure 4. Spectrum of brainstem trigeminal fiber microstructural alterations. Mean DTI metrics (±SEM) of responders (green) and nonresponders (red) across the subtypes of TN. (A–D) Responder subgroups of CTN and MS-TN do not show significant differences across all 4 DTI metrics. (E–H) Nonresponder subgroups of CTN, MS-TN, and SPL-TN show a significant gradient of brainstem trigeminal fiber microstructural abnormalities, where changes in FA are the most notable (E), followed by RD (F) and MD (G). No differences were found in AD (H). $^{*}P < 0.05$, $^{**}P < 0.01$, $^{***}P < 0.001$, $^{****}P < 0.0001$ (multiple comparison corrected). AD, axial diffusivity; CTN, classical TN; DTI, diffusion tensor imaging; FA, fractional anisotropy; MD, mean diffusivity; MS-TN, TN secondary to multiple sclerosis; RD, radial diffusivity; SPL-TN, TN associated with solitary pontine lesion; TN, trigeminal neuralgia.

a clinical response spectrum across the subtypes of TN, where CTN patients have the highest surgical response rate, followed by MS-TN patients, and, finally, SPL-TN patients, and (3) this clinical response spectrum is associated with the degree of brainstem trigeminal fiber microstructural abnormalities (**Fig. 6**). Thus, our study demonstrates the value of DTI as an objective, noninvasive tool for the prediction of treatment response and elucidates the neuroanatomical features that distinguish treatment responders from nonresponders in the TN population. On a broader scope, neuroimaging-based predictive biomarkers for pain are gaining

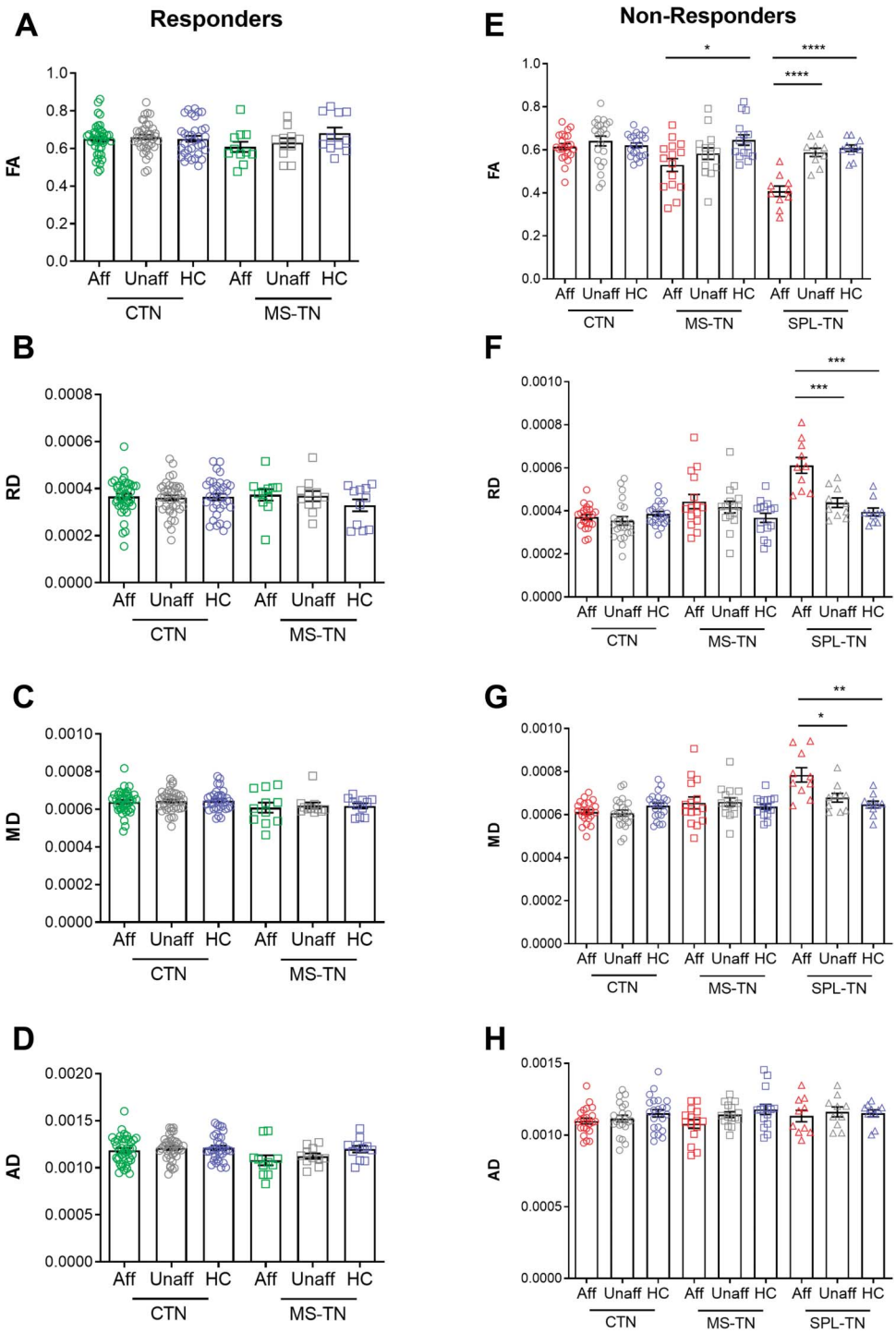

Figure 5. Brainstem trigeminal fiber microstructural alterations compared with controls. Mean DTI metrics (±SEM) of the affected side (green, responders; red, nonresponders), unaffected side (grey), and healthy controls (blue). (A–D) Microstructural characteristics of the affected side, unaffected side, and healthy controls do not significantly differ from each other in both responder subgroups of CTN and MS-TN. (E–H) Reflecting the gradient of brainstem trigeminal fiber microstructural abnormalities across the nonresponder subgroups, MS-TN nonresponders show significantly lower FA on the affected side compared with healthy controls (E, middle), whereas SPL-TN nonresponders show significantly lower FA (E, right), and higher RD (F, right) and MD (G, right) on the affected side compared with the unaffected side and healthy controls. CTN nonresponders do not show significant differences across all comparisons. $^{*}P < 0.05$, $^{**}P < 0.01$, $^{***}P < 0.001$, $^{****}P < 0.0001$ (multiple comparison corrected). AD, axial diffusivity; Aff, affected side; CTN, classical TN; DTI, diffusion tensor imaging; FA, fractional anisotropy; HC, healthy controls; MD, mean diffusivity; MS-TN, TN secondary to multiple sclerosis; RD, radial diffusivity; SPL-TN, TN associated with solitary pontine lesion; Unaff, unaffected side.

traction.[24,38] As such, this study builds an important framework towards individualized prediction in the pain field and additional tools that can be used to help advise chronic pain patients on their potential outcomes in the clinic.

Major advances in DTI methods have allowed more sophisticated approaches to better study TN and its neuroanatomical signatures. The first collection of such studies demonstrated white matter microstructural abnormalities at the affected

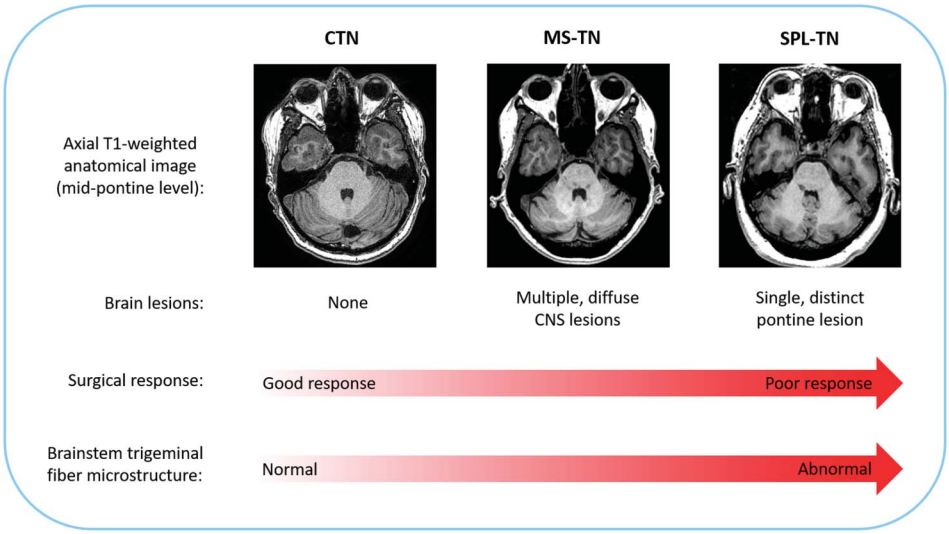

Figure 6. Schematic illustration of study findings and conclusion. Patients with CTN, MS-TN, and SPL-TN have distinct radiological features, as determined by the presence and extent of lesion(s). These features likely affect surgical outcome because of the following study findings: (1) there is a gradient of surgical response across the subtypes of TN (CTN → MS-TN → SPL-TN) and (2) the spectrum of surgical response is associated with the degree of brainstem trigeminal fiber microstructural abnormalities. CNS, central nervous system; CTN, classical TN; MS-TN, TN secondary to multiple sclerosis; SPL-TN, TN associated with solitary pontine lesion; TN, trigeminal neuralgia.

trigeminal root entry zone, characterized by lower FA,[5,13,20,22] and higher MD, RD, and AD.[5] These findings were followed by the development of XST, which allowed successful delineation and quantitative microstructural assessment of the central (brainstem) components of the trigeminal nerve pathway in patients with CTN[16] and MS-TN.[3] White matter abnormalities in higher brain areas have also been revealed using DTI, where TN patients demonstrate alterations in white matter pathways linked to cortical regions implicated in the multidimensional experience of pain, including sensory, affective, and cognitive dimensions.[5,10,41] Overall, these foundational studies have demonstrated the ability of DTI to investigate structural abnormalities of TN that cannot be distinguished on conventional MRI. These advanced methods have more recently carried forward into the clinical setting, where studies have investigated the translational, clinical value of DTI to advance personalized patient care. In TN, DTI has been shown to detect focal microstructural changes at the surgical target of the trigeminal nerve after GKRS treatment.[15] Moreover, sufficient microstructural changes (in particular, reductions in FA) at the target have been shown to predict long-term clinical effectiveness[36] and be a persistent, longitudinal biomarker of long-lasting pain relief.[17] These findings elucidate the mechanisms of GKRS treatment and the role of DTI in the clinical management of TN patients.

Here, we used DTI in the context of treatment response prediction and found that DTI metrics of the affected brainstem trigeminal fibers differentiate responders from nonresponders in a large, mixed cohort of TN patients. Specifically, nonresponders demonstrated significantly lower FA and AD, and higher RD, compared with responders and healthy controls at the proximal pontine segment of the trigeminal nerve. Responders showed no diffusivity differences compared with healthy controls. These findings suggest that patients with centrally driven microstructural alterations are less likely to respond to surgical treatment compared with patients who demonstrate a normal trigeminal brainstem diffusivity profile. Previous studies that have investigated microstructural features of surgical response in TN examined pretreatment imaging measures at 3 distinct anatomical sites along the trigeminal nerve: the cisternal segment, root entry zone, and pontine segment.[16,21] Hung et al.[16] studied patients with CTN and found abnormal pontine trigeminal fibers, characterized by higher AD, to be a key feature of nonresponders. Li et al.[21] examined patients with MS-TN, and also found abnormal pontine trigeminal fibers to be characteristic of nonresponders, distinguished by decreased myelin mapping intensities (ie, lower myelin content). Furthermore, a newly defined subtype of TN, called SPL-TN, consisting of nonresponders also demonstrated abnormal pontine trigeminal fibers, characterized by lower FA, and higher MD, RD, and AD.[37] Taken together, these isolated studies investigating the microstructural patterns of surgical response in specific subtypes of TN all point to abnormalities in more central components of the trigeminal nerve pathway—specifically, the brainstem trigeminal fibers—as a significant feature of treatment nonresponse. The results of the current study demonstrate that this is indeed a common characteristic of treatment nonresponse in a large cohort of TN patients, consisting of all 3 subtypes. It is the largest study to date that has examined the role of DTI in the prediction of treatment response for TN.

The second part of our study examined the specific subtypes of TN and found a clear gradient of treatment response across the 3 groups. Specifically, CTN patients had the highest response rate to surgical treatment, followed by MS-TN patients, and, finally, SPL-TN patients. This trend reflects the surgical outcomes reported in the literature.[7,8,14,19,26,28,32,37,40,42] Furthermore, we examined DTI metrics of the brainstem trigeminal fibers across the subtype-response groups and found that the degree of microstructural abnormalities on the affected side is associated with the likelihood of surgical response. Notably, SPL-TN nonresponders showed the greatest degree of microstructural abnormalities, characterized by lower FA, and higher RD and MD, followed by MS-TN patients, and, finally, CTN patients. Classical TN and MS-TN responders did not reveal any differences across the 4 metrics. These findings show that

the type of TN and the extent of microstructural disruption of the central trigeminal pathway are important factors that are associated with the likelihood of surgical response in TN.

The brainstem trigeminal fiber microstructural abnormalities we found likely stem from the presence and extent of lesions along the trigeminal brainstem pathway. Classical TN patients typically do not present with any brain lesions and, with the exception of neurovascular compression, demonstrate normal findings on conventional MRI. On the other hand, MS-TN patients typically present with multiple, demyelinating brainstem plaques, which has been attributed to the severe, paroxysmal pain.[4] These plaques often appear along the trigeminal pontine pathway and have been shown to disrupt the diffusivity of coinciding trigeminal fibers.[3] Multiple sclerosis plaques, however, are more diffuse and less demarcated compared with SPL-TN lesions.[37] On a T1-weighted image, a SPL-TN lesion appears much more prominent and hypointense (ie, like a "black hole"). As such, SPL-TN lesions have been shown to demonstrate greater disruption of the brainstem trigeminal fiber microstructure compared with MS plaques.[37] Taken together, the presence and extent of lesions across the subtypes of TN likely corresponds to the degree of brainstem trigeminal fiber microstructural abnormalities and subsequent likelihood of response to treatment demonstrated in this study (**Fig. 6**). This information may be valuable in the clinical setting to guide therapeutic strategies. For example, physicians may counsel patients who may not benefit from conventional surgical treatments to seek alternative therapies, such as neuromodulation, for optimal outcome.

Overall, among the 4 DTI metrics, we found FA to be the best biomarker of surgical response in TN. Fractional anisotropy is the most commonly used DTI metric to characterize white matter microstructure and has been shown to be a strong prognostic indicator of clinical progression and treatment response in a number of pathological disorders.[1] In CTN patients, FA has been shown to be a key biomarker of successful long-term pain relief, specifically at the surgical target after GKRS treatment.[17,36] Although, other DTI metrics, such as AD, which is more specific to axonal damage, has also been shown to be altered at the pontine segment in CTN nonresponders before treatment.[16] In the current study, we also found RD to be a strong biomarker of surgical response in TN. This suggests that the microstructural disruption observed in nonresponders may be mainly because of changes in myelination (ie, demyelination). These findings provide insight into the potential underlying pathophysiological mechanisms that differentiate responders from nonresponders to surgical treatment in TN.

We note several limitations to our study. First, the surgical technique used varied across patients, including MVD, GKRS, and PTR. Because each treatment targets a different portion of the trigeminal nerve by disparate mechanisms, it may be important for future studies to examine these treatment approaches separately to better understand the underlying mechanisms. Second, our study has the common limitations of a retrospective study. As an important future direction, a larger prospective study may enable the construction of a generalizable multivariate machine learning model that can be used to predict treatment response at the individual level.

In conclusion, our study brings together many of the central findings from extant neuroimaging studies of TN, which are the following: (1) DTI can be used to study the structural abnormalities of TN (in particular, the trigeminal nerve) that cannot be distinguished on conventional MRI, (2) DTI has a translational, clinical value for the assessment of neurosurgical response in TN, and (3) centrally disrupted brainstem trigeminal fibers is a key characteristic of treatment nonresponders in TN. Our novel findings demonstrate that abnormal brainstem trigeminal fiber microstructure is indeed a common characteristic of treatment nonresponse across different subtypes of TN and that the extent of these abnormalities is associated with the likelihood of response. Thus, DTI holds the promise of advancing patient care for TN patients by serving as an objective, noninvasive, clinically translatable tool to study TN pain and its treatment outcomes.

Conflict of interest statement

The authors have no conflicts of interest to declare.

Acknowledgements

This work was supported by the Canadian Institutes of Health Research (operating grant to M.H., Ref. # MOP130555). S.Tohyama is the recipient of the Canadian Institutes of Health Research Doctoral Research Award (Ref. # GSD164127).

Article history:
Received 24 August 2020
Received in revised form 29 October 2020
Accepted 17 November 2020
Available online 3 December 2020

References

[1] Alexander AL, Lee JE, Lazar M, Field AS. Diffusion tensor imaging of the brain. Neurotherapeutics 2007;4:316–29.
[2] Behan B, Chen DQ, Sammartino F, DeSouza DD, Wharton-Shukster E, Hodaie M. Comparison of diffusion-weighted MRI reconstruction methods for visualization of cranial nerves in posterior fossa surgery. Front Neurosci 2017;11:554.
[3] Chen DQ, DeSouza DD, Hayes DJ, Davis KD, O'Connor P, Hodaie M. Diffusivity signatures characterize trigeminal neuralgia associated with multiple sclerosis. Mult Scler 2016;22:51–63.
[4] Cruccu G, Biasiotta A, Di Rezze S, Fiorelli M, Galeotti F, Innocenti P, Mameli S, Millefiorini E, Truini A. Trigeminal neuralgia and pain related to multiple sclerosis. PAIN 2009;143:186–91.
[5] DeSouza DD, Hodaie M, Davis KD. Abnormal trigeminal nerve microstructure and brain white matter in idiopathic trigeminal neuralgia. PAIN 2014;155:37–44.
[6] DeSouza DD, Davis KD, Hodaie M. Reversal of insular and microstructural nerve abnormalities following effective surgical treatment for trigeminal neuralgia. PAIN 2015;156:1112–23.
[7] Dhople AA, Adams JR, Maggio WW, Naqvi SA, Regine WF, Kwok Y. Long-term outcomes of Gamma Knife radiosurgery for classic trigeminal neuralgia: implications of treatment and critical review of the literature. Clinical article. J Neurosurg 2009;111:351–8.
[8] Di Stefano G, Maarbjerg S, Truini A. Trigeminal neuralgia secondary to multiple sclerosis: from the clinical picture to the treatment options. J Headache Pain 2019;20:20.
[9] Fedorov A, Beichel R, Kalpathy-Cramer J, Finet J, Fillion-Robin JC, Pujol S, Bauer C, Jennings D, Fennessy F, Sonka M, Buatti J, Aylward S, Miller JV, Pieper S, Kikinis R. 3D slicer as an image computing platform for the Quantitative Imaging Network. Magn Reson Imaging 2012;30:1323–41.
[10] Hayes DJ, Chen DQ, Zhong J, Lin A, Behan B, Walker M, Hodaie M. Affective circuitry alterations in patients with trigeminal neuralgia. Front Neuroanat 2017;11:73.
[11] Headache Classification Committee of the International Headache Society (IHS). The International Classification of Headache Disorders, 3rd edition (beta version). Cephalalgia 2013;33:629–808.
[12] Headache Classification Committee of the International Headache Society (IHS). The International Classification of Headache Disorders, 3rd edition. Cephalalgia 2018;38:1–211.
[13] Herweh C, Kress B, Rasche D, Tronnier V, Troger J, Sartor K, Stippich C. Loss of anisotropy in trigeminal neuralgia revealed by diffusion tensor imaging. Neurology 2007;68:776–8.

[14] Hodaie M, Coello AF. Advances in the management of trigeminal neuralgia. J Neurosurg Sci 2013;57:13–21.
[15] Hodaie M, Chen DQ, Quan J, Laperriere N. Tractography delineates microstructural changes in the trigeminal nerve after focal radiosurgery for trigeminal neuralgia. PLoS One 2012;7:e32745.
[16] Hung PS, Chen DQ, Davis KD, Zhong J, Hodaie M. Predicting pain relief: use of pre-surgical trigeminal nerve diffusion metrics in trigeminal neuralgia. Neuroimage Clin 2017;15:710–18.
[17] Hung PS, Tohyama S, Zhang JY, Hodaie M. Temporal disconnection between pain relief and trigeminal nerve microstructural changes after Gamma Knife radiosurgery for trigeminal neuralgia. J Neurosurg 2019. doi: 10.3171/2019.4.JNS19380 [Epub ahead of print].
[18] Jenkinson M, Beckmann CF, Behrens TE, Woolrich MW, Smith SM. FSL. Neuroimage 2012;62:782–90.
[19] Kondziolka D, Zorro O, Lobato-Polo J, Kano H, Flannery TJ, Flickinger JC, Lunsford LD. Gamma Knife stereotactic radiosurgery for idiopathic trigeminal neuralgia. J Neurosurg 2010;112:758–65.
[20] Leal PR, Roch JA, Hermier M, Souza MA, Cristino-Filho G, Sindou M. Structural abnormalities of the trigeminal root revealed by diffusion tensor imaging in patients with trigeminal neuralgia caused by neurovascular compression: a prospective, double-blind, controlled study. PAIN 2011; 152:2357–64.
[21] Li CMF, Hung PS, Chu PP, Tohyama S, Hodaie M. Trigeminal neuralgia associated with multiple sclerosis: a multimodal assessment of brainstem plaques and response to Gamma Knife radiosurgery. Mult Scler 2020;26: 1877–88.
[22] Lutz J, Linn J, Mehrkens JH, Thon N, Stahl R, Seelos K, Bruckmann H, Holtmannspotter M. Trigeminal neuralgia due to neurovascular compression: high-spatial-resolution diffusion-tensor imaging reveals microstructural neural changes. Radiology 2011;258:524–30.
[23] Maarbjerg S, Wolfram F, Gozalov A, Olesen J, Bendtsen L. Significance of neurovascular contact in classical trigeminal neuralgia. Brain 2015;138(pt 2):311–19.
[24] Mackey S, Greely HT, Martucci KT. Neuroimaging-based pain biomarkers: definitions, clinical and research applications, and evaluation frameworks to achieve personalized pain medicine. Pain Rep 2019;4:e762.
[25] Meaney JF, Watt JW, Eldridge PR, Whitehouse GH, Wells JC, Miles JB. Association between trigeminal neuralgia and multiple sclerosis: role of magnetic resonance imaging. J Neurol Neurosurg Psychiatry 1995;59: 253–9.
[26] Moreno NEM, Gutiérrez-Sárraga J, Rey-Portolés G, Jiménez-Huete A, Álvarez RM. Long-term outcomes in the treatment of classical trigeminal neuralgia by Gamma knife radiosurgery: a retrospective study in patients with minimum 2-year follow-up. Neurosurgery 2016; 79:879–88.
[27] Nurmikko TJ, Eldridge PR. Trigeminal neuralgia—pathophysiology, diagnosis and current treatment. Br J Anaesth 2001;87:117–32.
[28] Obermann M. Treatment options in trigeminal neuralgia. Ther Adv Neurol Disord 2010;3:107–15.
[29] O'Donnell LJ, Westin CF. An introduction to diffusion tensor image analysis. Neurosurg Clin N Am 2011;22:185–96, viii.
[30] Peled S, Friman O, Jolesz F, Westin CF. Geometrically constrained two-tensor model for crossing tracts in DWI. Magn Reson Imaging 2006;24: 1263–70.
[31] Qazi AA, Radmanesh A, O'Donnell L, Kindlmann G, Peled S, Whalen S, Westin CF, Golby AJ. Resolving crossings in the corticospinal tract by two-tensor streamline tractography: method and clinical assessment using fMRI. Neuroimage 2009;47:T98–T106.
[32] Regis J, Tuleasca C, Resseguier N, Carron R, Donnet A, Gaudart J, Levivier M. Long-term safety and efficacy of Gamma Knife surgery in classical trigeminal neuralgia: a 497-patient historical cohort study. J Neurosurg 2016;124:1079–87.
[33] Song SK, Sun SW, Ramsbottom MJ, Chang C, Russell J, Cross AH. Dysmyelination revealed through MRI as increased radial (but unchanged axial) diffusion of water. Neuroimage 2002;17:1429–36.
[34] Song SK, Sun SW, Ju WK, Lin SJ, Cross AH, Neufeld AH. Diffusion tensor imaging detects and differentiates axon and myelin degeneration in mouse optic nerve after retinal ischemia. Neuroimage 2003;20:1714–22.
[35] Song SK, Yoshino J, Le TQ, Lin SJ, Sun SW, Cross AH, Armstrong RC. Demyelination increases radial diffusivity in corpus callosum of mouse brain. Neuroimage 2005;26:132–40.
[36] Tohyama S, Hung PS, Zhong J, Hodaie M. Early postsurgical diffusivity metrics for prognostication of long-term pain relief after Gamma Knife radiosurgery for trigeminal neuralgia. J Neurosurg 2018;131:539–48.
[37] Tohyama S, Hung PS, Cheng JC, Zhang JY, Halawani A, Mikulis DJ, Oh J, Hodaie M. Trigeminal neuralgia associated with a solitary pontine lesion: clinical and neuroimaging definition of a new syndrome. PAIN 2020;161:916–25.
[38] van der Miesen MM, Lindquist MA, Wager TD. Neuroimaging-based biomarkers for pain: state of the field and current directions. Pain Rep 2019;4:e751.
[39] Willsey MS, Collins KL, Conrad EC, Chubb HA, Patil PG. Diffusion tensor imaging reveals microstructural differences between subtypes of trigeminal neuralgia. J Neurosurg 2019. doi: 10.3171/2019.4.JNS19299 [Epub ahead of print].
[40] Xu Z, Mathieu D, Heroux F, Abbassy M, Barnett G, Mohammadi AM, Kano H, Caruso J, Shih HH, Grills IS, Lee K, Krishnan S, Kaufmann AM, Lee JYK, Alonso-Basanta M, Kerr M, Pierce J, Kondziolka D, Hess JA, Gerrard J, Chiang V, Lunsford LD, Sheehan JP. Stereotactic radiosurgery for trigeminal neuralgia in patients with multiple sclerosis: a multicenter study. Neurosurgery 2019;84:499–505.
[41] Zhong J, Chen DQ, Hung PS, Hayes DJ, Liang KE, Davis KD, Hodaie M. Multivariate pattern classification of brain white matter connectivity predicts classic trigeminal neuralgia. PAIN 2018;159:2076–87.
[42] Zorro O, Lobato-Polo J, Kano H, Flickinger JC, Lunsford LD, Kondziolka D. Gamma knife radiosurgery for multiple sclerosis-related trigeminal neuralgia. Neurology 2009;73:1149–54.